Original Article

Defined MSC exosome with high yield and purity to improve regenerative activity

Journal of Tissue Engineering
Volume 12: 1–15
© The Author(s) 2021
Article reuse guidelines:
sagepub.com/journals-permissions
DOI: 10.1177/20417314211008626
journals.sagepub.com/home/tej
SAGE

Jun Yong Kim[1,2,3*], Won-Kyu Rhim[1*], Yong-In Yoo[1], Da-Seul Kim[1,4], Kyoung-Won Ko[1], Yun Heo[1], Chun Gwon Park[2,3] and Dong Keun Han[1]

Abstract

Exosomes derived from mesenchymal stem cells (MSCs) have been studied as vital components of regenerative medicine. Typically, various isolation methods of exosomes from cell culture medium have been developed to increase the isolation yield of exosomes. Moreover, the exosome-depletion process of serum has been considered to result in clinically active and highly purified exosomes from the cell culture medium. Our aim was to compare isolation methods, ultracentrifuge (UC)-based conventional method, and tangential flow filtration (TFF) system-based method for separation with high yield, and the bioactivity of the exosome according to the purity of MSC-derived exosome was determined by the ratio of Fetal bovine serum (FBS)-derived exosome to MSC-derived exosome depending on exosome depletion processes of FBS. The TFF-based isolation yield of exosome derived from human umbilical cord MSC (UCMSC) increased two orders (92.5 times) compared to UC-based isolation method. Moreover, by optimizing the process of depleting FBS-derived exosome, the purity of UCMSC-derived exosome, evaluated using the expression level of MSC exosome surface marker (CD73), was about 15.6 times enhanced and the concentration of low-density lipoprotein-cholesterol (LDL-c), known as impurities resulting from FBS, proved to be negligibly detected. The wound healing and angiogenic effects of highly purified UCMSC-derived exosomes were improved about 23.1% and 71.4%, respectively, with human coronary artery endothelial cells (HCAEC). It suggests that the defined MSC exosome with high yield and purity could increase regenerative activity.

Keywords

Exosome, mesenchymal stem cell (MSC), isolation yield, purity, angiogenesis, wound healing

Date Received: 3 February 2021; accepted: 21 March 2021

[1]Department of Biomedical Science, CHA University, Seongnam, Gyeonggi, Republic of Korea
[2]Department of Biomedical Engineering, SKKU Institute for Convergence, Sungkyunkwan University (SKKU), Suwon, Gyeonggi, Republic of Korea
[3]Department of Intelligent Precision of Healthcare Convergence, SKKU Institute for Convergence, Sungkyunkwan University (SKKU), Suwon, Gyeonggi, Republic of Korea
[4]School of Integrative Engineering, Chung-Ang University, Seoul, Republic of Korea

*These authors equally contributed to this work.

Corresponding author:
Dong Keun Han, Department of Biomedical Science, CHA University, 335 Pangyo-ro, Bundang-gu, Seongnam, Gyeonggi 13488, Republic of Korea.
Email: dkhan@cha.ac.kr

Creative Commons Non Commercial CC BY-NC: This article is distributed under the terms of the Creative Commons Attribution-NonCommercial 4.0 License (https://creativecommons.org/licenses/by-nc/4.0/) which permits non-commercial use, reproduction and distribution of the work without further permission provided the original work is attributed as specified on the SAGE and Open Access pages (https://us.sagepub.com/en-us/nam/open-access-at-sage).

Introduction

Mesenchymal stem cells (MSCs) have widely been used for therapeutic treatments in many preclinical models of immunological and degenerative diseases.[1–5] These therapeutic effects of MSCs result from transdifferentiation of stem cells, cell fusion, mitochondrial transfer, and paracrine effects of cells.[6,7] Paracrine factors, including chemokines, cytokines, and growth factors, have recently been widely studied with extensive use of MSCs in clinical trials.[8] In particular, extracellular vesicles (EVs) have been recognized as an important bioactive component for paracrine effects of MSCs.[9,10]

Small vesicular particles with a lipid bilayer called EVs are cell-secreted nanovesicles that facilitate intercellular communications by exchanging proteins, lipids, and RNA between cells.[11–14] EVs are categorized into different subtypes, microvesicles, apoptotic bodies, and exosomes, based on their subcellular origin, biogenesis, size, and molecular compositions.[15] It is now widely accepted that exosomes are secreted by multivesicular bodies (MVBs) with 40–150 nm size.[16,17] The characteristics of secreted exosomes vary depending on origins, type, and condition of parent cells.[18] It can be used as an alternative to cell-based therapy that retains the characteristics of the original cells. In particular, MSC-derived exosomes can be applied to various regenerative medicine, including angiogenesis and wound repair,[19,20] alleviating liver fibrosis,[21] cardiac repair,[22] neurodegeneration treatment,[23] and osteochondral regeneration.[24] However, there are still barriers to the widespread development of MSC exosome-based therapies for human patients.

With increasing potential for their clinical use, optimizing their isolation processes for maximum yield and purity with biological activity has become essential. Common isolation methods for the separation of exosomes from the cell culture medium are ultracentrifugation (UC),[25] ultrafiltration (UF),[26] size exclusion chromatography (SEC),[27] polymer precipitation,[28] and density gradients (DG).[29] Ultracentrifugation method has been the "gold standard" for exosome isolation; however, it is limited by extremely low isolation yield and a high degree of protein aggregate and lipoprotein contamination in exosomes. Moreover, this method requires laborious repeated centrifugation steps to remove non-exosome proteins. In order to overcome this issue, a tangential flow filtration system (TFF) has been recently introduced for separating exosomes in a large volume of cell culture medium for a short time.[30] TFF is a filtration method that uses tangential flow across the surface, avoiding filter cake formation.[31] With optimum pore size of filter, small sized protein impurities are removed, and exosome can be efficiently isolated and concentrated.

In order to isolate the exosomes from a high purity cell culture medium, the composition of the cell culture medium is an essential factor to be considered. In the last 20 years, it has been confirmed that serum contains large amounts of exosomes without unraveling their function.[32,33] Besides, several reports on MSC-derived exosomes used exosome, which was isolated from a serum-containing cell culture medium. Considering that an enormous number of lipoprotein particles are present in serum,[34] the biological activity of MSC-derived exosomes decreases, and unknown side effects can occur without depletion processes for serum-derived exosomes.

In this study, the isolation yield and purity based on FBS-derived exosome depletion method in cell culture medium and isolation methods of UCMSC-derived exosome were comparatively analyzed. The distribution of exosome markers was compared based on the purity of MSC-derived exosomes and the subpopulations of exosomes were classified using principal component analysis (PCA). Moreover, the biological activity of the MSC-derived exosome has been demonstrated depending on the purity of UCMSC-derived exosomes.

Materials and methods

Exosome (EV) isolation

Human umbilical cord mesenchymal stem cells (UCMSCs; CHA Biotech Co. Ltd., Seongnam, Korea) were cultured up to approximately 50% confluence in alpha-MEM (HyClone laboratories, UT, USA) containing 1% antibiotic-antimycotic mixture (GIBCO, NY, USA) and 10% fetal bovine serum (FBS, HyClone laboratories, UT, USA) and maintained in a humidified atmosphere with 5% CO_2 at 37°C. Approximately 50% confluent cells were cultured for 48 h in phenol red-free DMEM (GIBCO, NY, USA) containing 1% antibiotic-antimycotic mixture and normal FBS (nFBS) or exosome depleted FBS using ultracentrifugation (UC-dFBS) or ultrafiltration (UF-dFBS). The UC-dFBS was obtained by nFBS ultracentrifugation for 18 h at 100,000*g* and 4°C (Optima L 100 XP, Beckman Coulter, CA, USA). UF-dFBS was obtained by nFBS filtration using Amicon Ultra-15 centrifugal filters (Millipore, Billerica, MA, USA) for 55 min at 3000*g*. Cell culture media were collected four times every 12 h for mass production of exosomes. The culture medium was centrifuged at 1300 rpm for 10 min and filtered through a 0.22 μm Vacuum Filter/Storage Bottle System (Corning, Cat. No. 431097) to remove large non-exosome particles, including cells, cell debris, microvesicles, and apoptotic bodies. Finally, exosomes were isolated using previous reported ultracentrifugation method[35] or a tangential flow filtration (TFF; Repligen, Waltham, MA, USA) system with a 300 or

500 kDa molecular weight cut-off filter for parallel comparisons.

Cell viability assay

After UCMSCs culture with nFBS, UC-dFBS, and UF-dFBS, cell viability was assessed with Cell Counting Kit-8 (CCK-8; Dojindo, Kumamoto, Japan). The CCK-8 assay was conducted according to instructions received from the manufacturer for determining the relative cell viability. Absorbance was measured using a microplate reader (Molecular Devices, CA, USA) at 450 nm wavelength.

Characterization of exosomes

The particle size and concentration were measured in 488 nm scatter mode with ZetaView QUATT® (Particle Metrix, Meerbusch, Germany). The samples were diluted in filtered phosphate-buffered saline (PBS) solution to concentrate 10^7–10^8 particles/ml. The detailed settings for accurate analysis were optimized with sensitivity 75, shutter 100, minimum trace length 15, and cell temperature 25°C for all samples. The tetraspanin subpopulations of exosomes were measured using ExoView™ (NanoView Biosciences, MA, USA). The sample concentration was diluted to 10^7–10^8 particles/ml using solution A of ExoView™ tetraspanin kit. The diluted exosome samples were dropped onto the tetraspanin chips and incubated for 16 h. After incubation, the chips were incubated with fluorescently labeled CD81, CD63, CD9 antibodies for 1 h. The absorbances of samples were analyzed using ExoView® R100 at 640, 555, and 488 nm wavelength. The structure of exosome was observed using transmission electron microscopy (TEM; Hitachi, H-7600, 80 kV, Japan). The exosome solution was dried on the copper grid with 200 mesh carbon film (CF200-Cu, Electron Microscopy Sciences, USA). For negative staining of exosomes, filtered 7% uranyl acetate was dropped on the copper grid and dried. After rinsing and drying, the grid was placed on the grid box for imaging by TEM.

Western blot analysis

The protein concentration of exosome was determined using a Pierce™ BCA Protein Assay Kit (Pierce, IL, USA). The exosome proteins were subjected to 10% SDS-PAGE and transferred onto nitrocellulose membranes. After blocking with TBST solutions dissolved in 5% skim milk, exosome transferred membranes were sequentially incubated with the primary antibody of CD81 (Santa Cruz Biotechnology, CA, USA), CD73, CD63, and CD9 (Abcam, MA, USA) and HRP linked secondary antibodies. The blots were subjected to enhanced chemiluminescence (ECL) solution (GE Healthcare, WI, USA), which were visualized using ChemiDoc XRS+ and ImageLab software (Bio-Rad, CA, USA).

Low-density lipoprotein cholesterol (LDL-C) analysis

Calibration was performed with control serum I and II (Wako Pure Chemical Industries, Osaka, Japan) before the analysis. In order to access the concentration of LDL-C, exosomes were dissolved in deionized water (DW) and analyzed with a Hitachi 7020 automatic biochemistry analyzer (Hitachi, Tokyo, Japan) according to instructions received from the manufacturer.

Fourier transform infrared (FTIR) measurement

All exosome samples were dissolved in DW for FTIR analysis with FTIR spectrum two (PerkinElmer, CT, USA) in transmission mode. Exosomes were dropped onto a calcium fluoride window and dried under a stream of nitrogen for 15 min. All FTIR spectra of exosomes were recorded in the wavenumber range of 900–4000 cm^{-1}, with a spectral resolution of 4 cm^{-1} and 32 scans. A background scan was performed using a DW-loaded calcium fluoride window.

Principal component analysis (PCA)

The spectra data were selected between 2800–3100 and 900–1880 cm^{-1} for principal component analysis (PCA) of exosomes.[8,36] The selected data were normalized by min-max normalization and centered using the mean subtraction method. PCA was performed by principal component analysis for spectroscopy application using OriginPro 2017 software (OriginLab, MA, USA).

Enzyme-linked immunosorbent assay (ELISA)

The expression level of angiogenic factors (VEGF, HGF, bFGF, and Angiopoietin-1) in exosomes was analyzed using the Quantikine™ ELISA kit (R&D Systems, MN, USA). The same amounts of exosomes (10 μg) were loaded in ELISA wells. The process of ELISA was conducted according to instructions received from the manufacturer. The absorbance was measured using a microplate reader at 450 nm wavelength.

Tube formation assay

Human coronary artery endothelial cells (HCAECs, 1.2×10^5 cells/well) were cultured with EGM-2 (Lonza, Basel, Switzerland) media on Matrigel-coated 24 well plates (Corning, NY, USA) for 17 h. The same concentration of exosomes (100 μg/ml) from various conditioned

medium was treated to the cultured cells. Subsequently, tube formation was imaged using fluorescence microscopy (CKX53, OLYMPUS, japan) after Calcein AM staining for cell visualization. Images were analyzed using the angiogenesis analyzer plugin of ImageJ software (Wayne Rasband, NIH, USA).

Cell migration assay

HCAECs (3×10^5 cells/well) were cultured with EGM-2 on six well plates. The cells were grown to confluent with a monolayer and scratched using a sterile 1 ml pipette tip in a straight line on the center of wells. The cells were washed and treated with the same concentration of exosomes (100 μg/ml) from various conditioned medium. After incubation for 24 h, the cell migration was imaged using a microscope. The percentage of wound closure was analyzed by the wound healing tool plugin of ImageJ software.

Statistical analysis

All statistical analyses were performed using GraphPad Prism 7 (GraphPad Software, CA, USA). Differences between groups were assessed using one-way analysis of variance (ANOVA) with Tukey's multiple comparison post-test and p values below 0.05 were considered as statistically significant (*$p < 0.05$; **$p < 0.01$; ***$p < 0.001$; ****$p < 0.0001$).

Results

Comparison of exosome isolation methods: Ultracentrifuge (UC) and tangential flow filtration (TFF) system

UCMSC-derived exosomes were isolated from the conditioned medium collected four times every 12 h. The more frequent collection of exosomes from the conditioned medium allows for an increase in total production yield without structural decomposition.[8] An equal volume of conditioned medium collected from the same number of UCMSCs was proceeded using conventional ultracentrifugation (UC) and tangential flow filtration (TFF) methods to directly compare the yield of exosome particles depending on isolation methods. The conditioned medium from MSC culture dishes was first purified through a 0.22 μm filter before the exosome isolation processes to remove large impurities (Figure 1(a)). In order to compare the production yield of isolated exosomes, the number of total particles was quantified using NTA (Figure 1(b)). Compared to UC, the TFF-based isolation method increased two orders of magnitude in exosome recovery from the same number of cells (0.02×10^{10} exosomes for UC and 1.85×10^{10} exosomes for TFF). Following the guideline of MISEV2018, exosomes isolated from UCMSC conditioned medium were characterized using Western blot analysis and TEM. The expression of exosome tetraspanins was observed by Western blot analysis (Figure 1(c)) from exosomes isolated using both UC and TFF systems. Double-layered spherical structures were observed using TEM (Figure 1(d)). With these results, it can be concluded that TFF is a scalable and productive method for obtaining exosomes from a cell culture medium compared to UC.

Filter membrane pore size-dependent exosome isolation yield in TFF system

It is widely accepted that multivesicular bodies secrete exosomes as 40–150 nm vesicles. Two different pore sizes of membrane filters were compared to optimize the pore size of TFF membrane filter for exosome isolation with higher purity. The conditioned medium, obtained four times in every 12 h from UCMSC cultured dish, was first passed through a 0.2 μm filter to remove large particles and then passed through a TFF filter membrane with two different membrane pore sizes of 300 and 500 kDa. By quantifying the isolated exosomes through two different TFF filters, a small amount of protein and a small number of particles were isolated using 500 kDa compared to 300 kDa (Figure 2(b)). It was expected due to the different cut-off ranges of two different filter sizes, as shown in Figure 2(a). The two groups of exosomes having similar size and structure were analyzed using NTA and TEM (Figure 2(c) and (d)), showing a similar distribution of representative exosome surface markers, CD9, CD63, and CD81, which were proved using Western blot analysis (Figure 2(e)) and ExoView™ analysis (Figure 2(f)). The exosome purity, determined by dividing the number of particles by a total protein amount,[37] is better when a 500 kDa filter is used (Figure 2(g)). The reason is that exosome smaller than 40 nm was separated using 500 kDa filter so that the yield could be less. Besides, purity can be increased as small non-exosomal impurities are removed more efficiently.

Exosome depletion processes for FBS

In cell experiments, FBS is used to supply nutrients for cell growth, although it is essential that FBS also contains significant amounts of exosomes. Besides, FBS-derived exosomes reduce the purity of exosomes from cells, affecting the distinction of exosome characteristics depending on the properties of cells. In order to solve this problem, two depletion methods of FBS-derived exosome have been compared: ultracentrifugation (UC) and ultrafiltration (UF). Ultracentrifugation, a conventional exosome depletion method from FBS to be processed for a long time at an ultrahigh-speed and ultrafiltration is a separation method of a relatively short time with a low speed using a

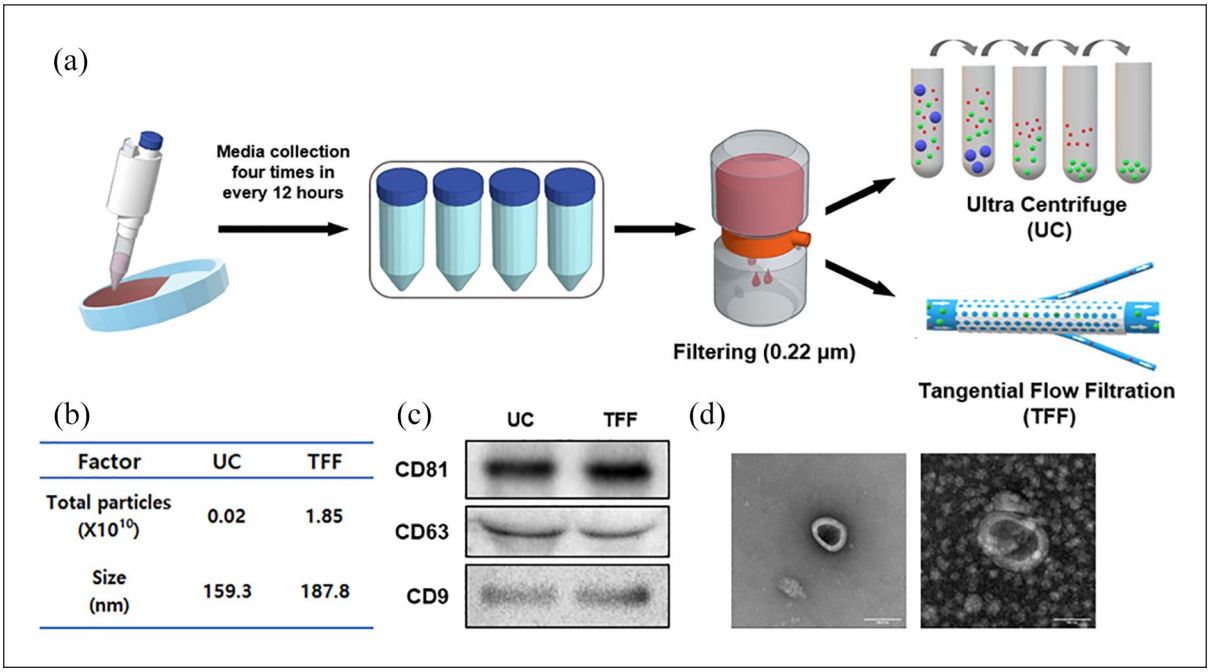

Figure 1. Isolation yield and characterization of MSC-derived exosome depending on isolation methods: (a) scheme of exosome isolation methods, (b) the table of total particles and size, (c) Western blotting analysis for the exosome surface markers; CD81, CD63, and CD9, and (d) TEM image of exosome. (Left. EV Isolated by ultracentrifuge, Right. EV Isolated by TFF). Scale bars 100 nm.

centrifugal filter (Figure 3(a)). Compared to normal FBS (nFBS), the number of exosomes present in the FBS was significantly reduced following the exosome depletion process of FBS. In particular, higher numbers of FBS-derived exosomes are removed by ultrafiltration compared to the ultracentrifugation process (Figure 3(b)). The size distribution of FBS-derived exosomes was compared based on depletion methods (Figure 3(c)).

UCMSC was cultured with the medium containing three different FBS to confirm the effect of depletion processes on cell viability (Figure 3(d)) (nFBS: normal FBS, UC-dFBS: exosome depleted FBS using ultracentrifugation, and UF-dFBS: exosome depleted FBS using ultrafiltration). Similar cell viability was observed in the cells using UC-dFBS and UF-dFBS, which was lower than using nFBS, but higher than without FBS (Starvation). From these results, it is proposed to use UF-dFBS to deplete FBS-derived exosomes efficiently with a proper cell viability of the cells.

Enhanced purity of UCMSC-derived exosome with optimized FBS-derived exosome depletion processes

In order to quantify the exosomes isolated from the UCMSC culture medium, the smallest number of exosomes was isolated from cells with the UF-dFBS medium (referred to as EXO_{SC}-UF-dFBS) (Figure 4(a) and (b)). However, the ratio of UCMSC-derived exosome was the highest in this condition (Figure 4(c)). The ratio of UCMSC-derived exosome was calculated by equation (1).

$$\left(\frac{Exo_{SC} - Exo_{FBS}}{Exo_{SC}}\right) \times 100 \quad (1)$$

Besides, the purity of UCMSC-derived exosomes, which was determined by dividing the number of particles by the amounts of proteins, was the highest in the same group (Figure 4(d)). To further compare the purity of the exosome isolated from the UCMSC culture medium, the expression intensity of CD73, one of the representative surface markers of MSC-derived exosomes, was analyzed using Western blot analysis. The results showed that the CD73 was highly expressed in EXO_{SC}-UF-dFBS compared to UCMSC-derived exosome culturing with nFBS (referred to as EXO_{SC}-nFBS) and UC-dFBS (referred to as EXO_{SC}-UC-dFBS) (Figure 4(e)). And the value for UCMSC exosome purity, that is, the intensity of CD73 divided by a number of particles, was the highest under the same condition (Figure 4(f)).

Meanwhile, low-density lipoprotein cholesterol (LDL-C) is contained in FBS and is considered impurities on UCMSC-derived exosomes.[38] Compared with EXO_{SC}-nFBS and

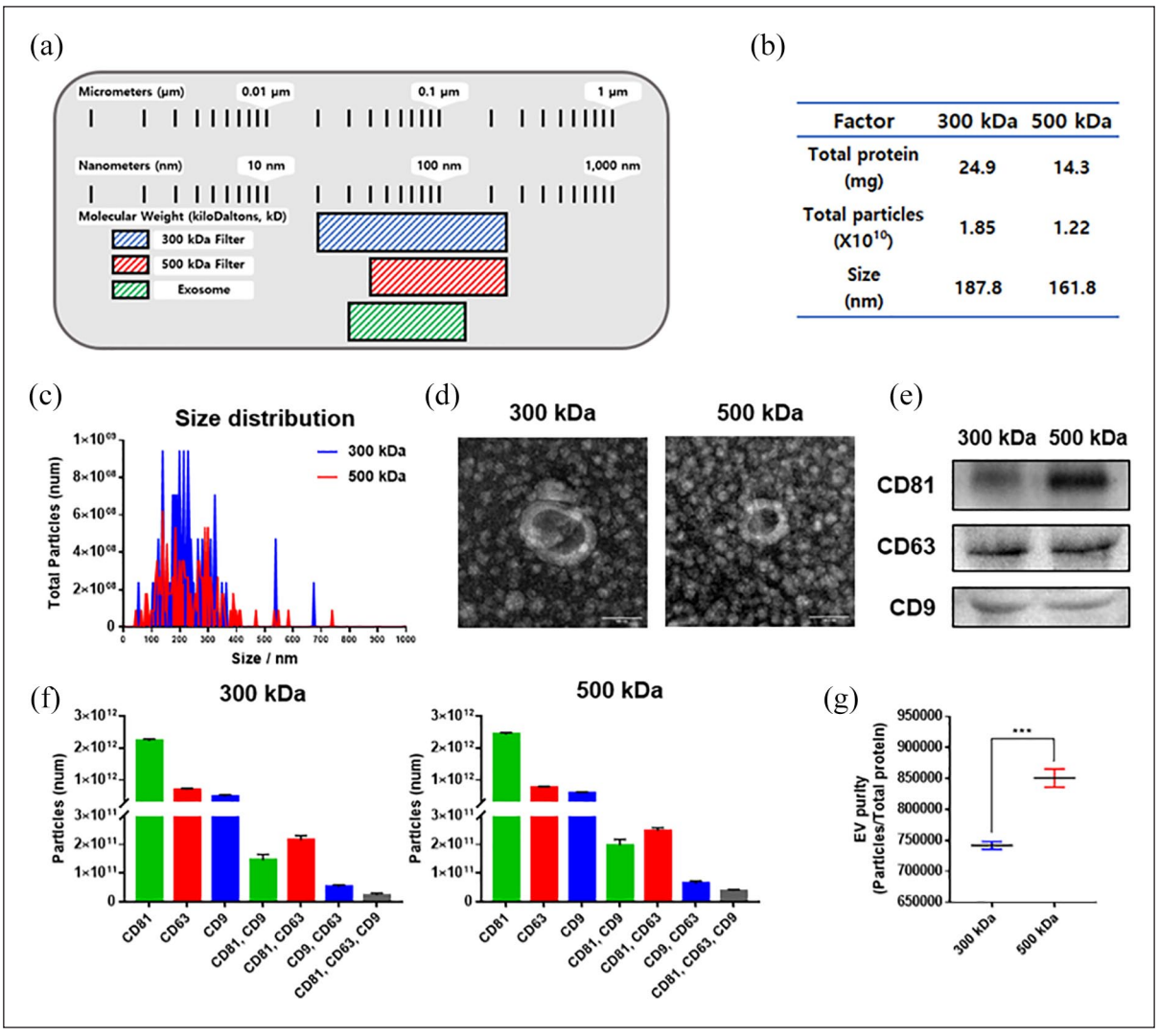

Figure 2. Filter pore size-dependent exosome production yield and purity using TFF system: (a) the range of each TFF filter cut-off size, (b) the table of total protein, particles, and size, (c) the particles concentration and the number of particles after TFF process (by NTA), (d) TEM image of exosome (Upper; 300 kDa Lower; 500 kDa [UC-FBS]), (e) Western blotting analysis for the exosome surface markers; CD81, CD63, and CD9, (f) tetraspanin tendency detected by ExoView-fluorescence, (g) purity of exosome. Scale bars 100 nm.

Values are presented as mean ± SD ($n = 3$) and statistical significance was obtained with oneway analysis of ANOVA with Tukey's multiple comparison post-test (***$p < 0.001$).

EXO_{SC}-UC-dFBS, much less LDL-C was detected in EXO_{SC}-UF-dFBS (Figure 4(g)). These results proved that UCMSC-derived exosomes could be separated with high purity in cell culture with UF-dFBS medium. The surface markers of the isolated exosomes using the medium under the three conditions, nFBS (EXO_{FBS}-nFBS), UC-dFBS (EXO_{FBS}-UC-dFBS), and UF-dFBS (EXO_{FBS}-UF-dFBS), were analyzed using Western blot analysis (Figure 4(h)), and the structures were observed using TEM (Figure 4(i)). Although the round-shaped structure with a bilayer was similar, it was confirmed that the expression intensity of each exosome tetraspanin differed depending on the condition of cell culture. ExoView™ analysis was performed to compare the expression level of exosome surface markers. The expression of CD9 increased, and the level of CD63 decreased as the ratio of UCMSC-derived exosome increased (Figure 4(j) and (k)). These results suggest that the properties of the isolated exosomes are different depending on the condition of cell culture medium.

The classification of exosome subpopulations using PCA converted by FTIR and zeta potential of exosomes

To distinguish subpopulations of exosomes based on the ratio of FBS-derived exosome and MSC-derived exosome,

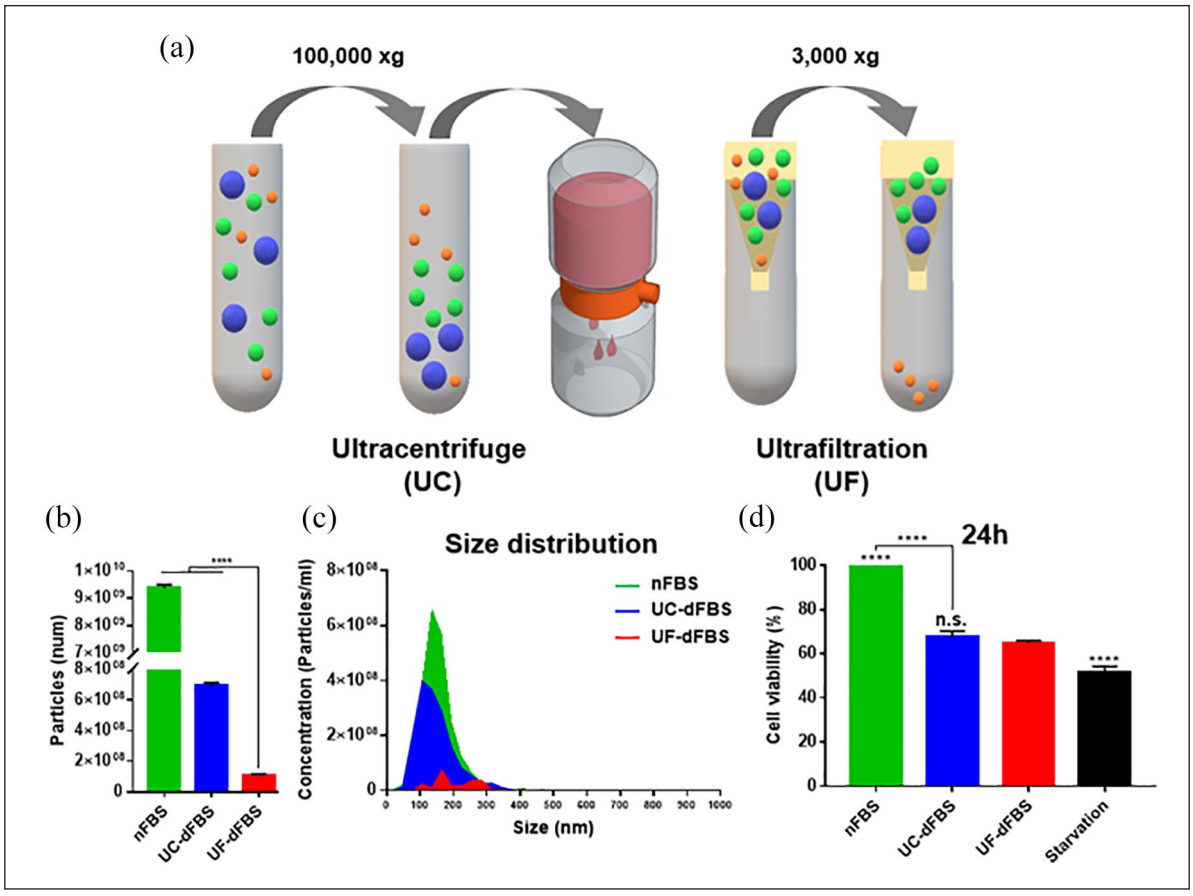

Figure 3. Comparison of the amount of FBS-derived exosome and cellular viability depending on FBS-derived exosome depletion method: (a) scheme of FBS exosome depletion method, (b) exosome particles concentration after exosome depletion process detected by NTA, (c) the size distribution of isolated exosome particles after exosome depletion process was detected by NTA, and (d) cell viability confirmed by CCK-8 solution.

nFBS: normal FBS; Starvation: without FBS; UC-dFBS: exosome-depleted FBS by ultracentrifuge; UF-dFBS: exosome-depleted FBS by ultrafiltration. Values are presented as mean ± SD ($n = 3$) and statistical significance was obtained with one-way analysis of ANOVA with Tukey's multiple comparison post-test (****$p < 0.0001$).

exosomes isolated from five different conditions were selected, including FBS-derived exosome in nFBS (EXO_{FBS}-nFBS), MSC-derived exosomes using nFBS medium (EXO_{SC}-nFBS), MSC-derived exosomes using UC-dFBS medium (EXO_{SC}-UC-dFBS), MSC-derived exosome using UF-dFBS medium (EXO_{SC}-UF-dFBS), and MSC-derived exosome in starvation condition (EXO_{SC}-Starvation). The principal components analysis (PCA) and zeta potential were utilized to classify subpopulations of exosome. To obtain PCA plots, representative IR spectra of different exosome subpopulations derived from FBS and UCMSC with various cell culture conditions are evaluated (Figure 5(a)). FTIR spectroscopy of biological systems provided information on the main biomolecules in a sample simultaneously, such as lipids, proteins, nucleic acids, and carbohydrates.[39] In this study, the specific absorption bands of lipid and proteins are characterized as biological properties directly associated with all exosome subpopulations. In particular, the amide I absorption band, around 1650 cm^{-1}, is due to the carbonyl stretching vibration, and the amide II absorption band, around 1540 cm^{-1}, is primarily owing to N–H bending vibrations.[40] Moreover, the range of spectrum between 2860–2940 cm^{-1} was characterized by the absorption of the lipid acyl chains, whereas the spectrum around 1740 cm^{-1} occurred by the absorption of the ester carbonyl groups.[41] These molecular vibrations are consistent with previous reports for exosome samples.[42,43] Subtle changes of the protein and lipid absorption region were observed, indicating that lipid and protein arrangement was changed depending on exosome subpopulations (Supplemental Figure S1). It is necessary to introduce a suitable multivariate method to distinguish these subtle differences. PCA is a multivariate statistical analysis that summarizes multiple parameters in one property, and it is applied for collective analysis with numerous parameters. PCA extracts valuable data, lipids, and proteins spectral regions from IR spectra in this case and visualizes them in a dimensional space. PCA score plots IR spectra (900–1880

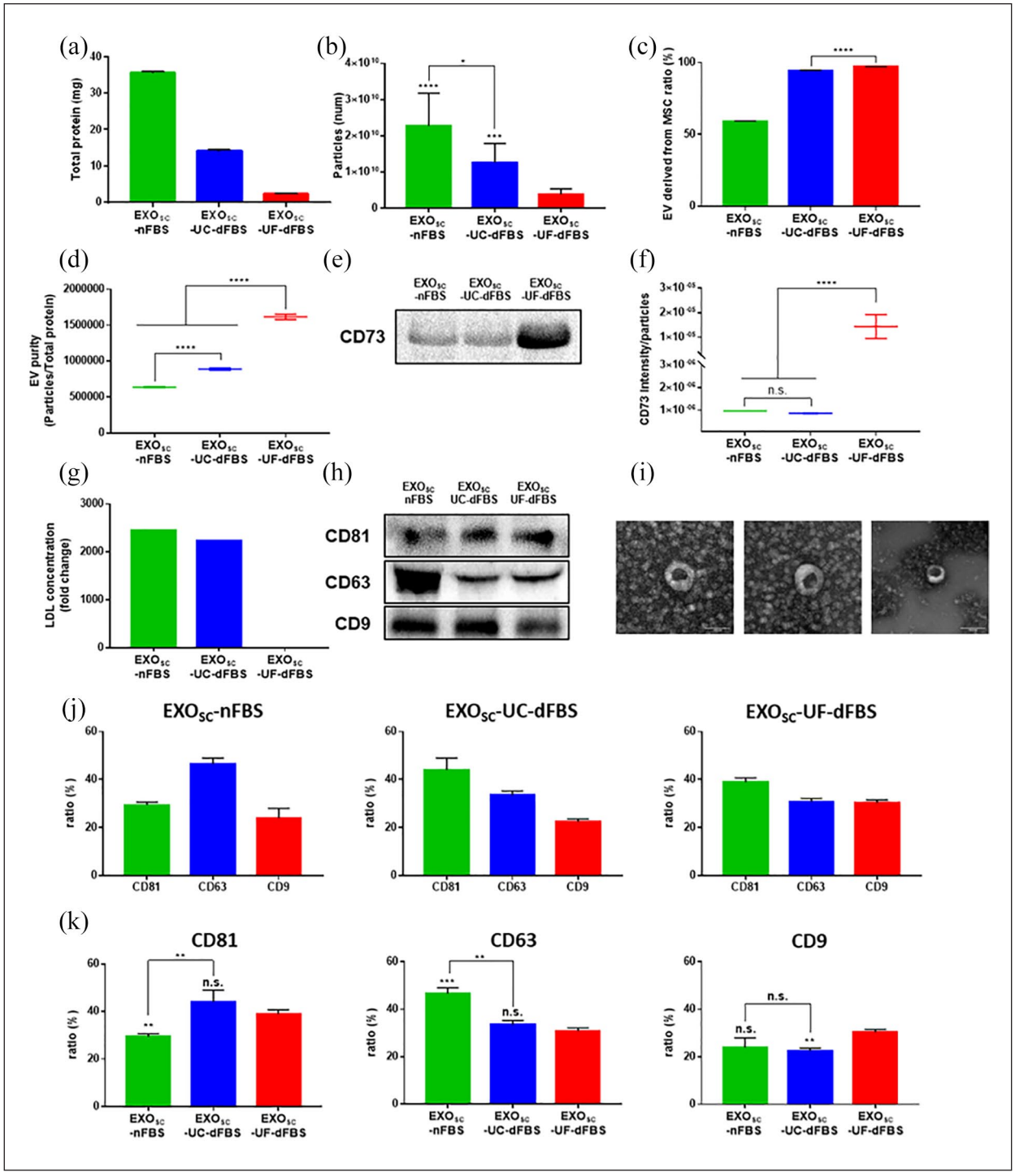

Figure 4. Characterization of MSC-derived exosomes using different exosome-depleted FBS-containing medium: (a) total proteins after exosome isolation process detected by BCA, (b) total particles after exosome isolation process detected by NTA, (c) the ratio of exosome derived from MSC, (d) the purity of MSC derived EV, (e) Western blotting analysis of CD73 MSC marker, (f) MSC-derived exosome purity calculated with CD73 intensity divided by the number of particles, (g) LDL concentration in isolated EV, (h) Western blotting analysis for the exosome surface markers; CD81, CD63, and CD9, (i) TEM image of exosome (Left; EXO_{SC}-nFBS Middle; EXO_{SC}-UC-dFBS Right; EXO_{SC}-UF-dFBS), (j) tetraspanin tendency detected by ExoView-fluorescence, and (k) tetraspanin ratio; CD81, CD63, CD9. Scale bars 100 nm.

EXO_{SC}-nFBS: MSC-derived exosome using nFBS medium; EXO_{SC}-UC-dFBS: MSC-derived exosome using UC-dFBS medium; EXO_{SC}-UF-dFBS: MSC-derived exosome using UF-dFBS medium.

Values are presented as mean ± SD ($n = 3$) and statistical significance was obtained with one-way analysis of ANOVA with Tukey's multiple comparison post-test (*$p < 0.05$; **$p < 0.01$; ***$p < 0.001$; ****$p < 0.0001$).

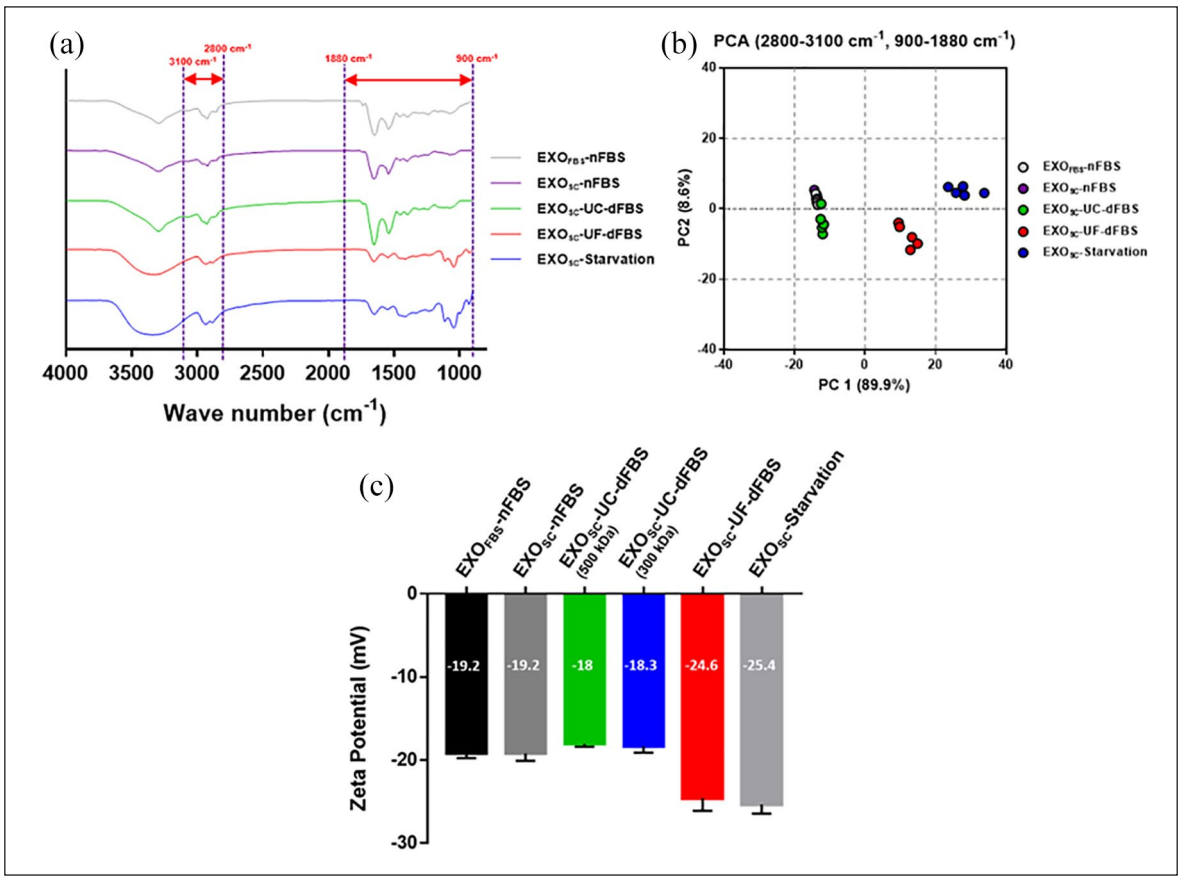

Figure 5. The classification of exosome subpopulations using PCA and zeta potential: (a) the FTIR spectra of the exosome in the wavenumber range of 900–4000 cm^{-1}, (b) the PCA score plot was described exosomes derived from different conditions. EXO_{FBS}-nFBS are shown by gray color, EXO_{SC}-nFBS by purple, EXO_{SC}-UC-dFBS by green, EXO_{SC}-UF-dFBS by red, and EXO_{SC}-Starvation by blue, and (c) zeta potential of exosomes in various conditions.
EXO_{FBS}-nFBS: FBS-derived exosome in nFBS; EXO_{SC}-Starvation: MSC-derived exosome in starvation condition (without FBS).

and 2800–3100 cm^{-1}) collected from exosomes, showing different exosome subpopulations from different conditioning medium (Figure 5(b), Purple: EXO_{SC}-nFBS, Green: EXO_{SC}-UC-dFBS, Red: EXO_{SC}-UF-dFBS). In order to compare the trends according to the subpopulation of exosomes, the FBS-derived exosome (EXO_{FBS}-nFBS) and the UCMSC-derived exosome in starvation (EXO_{SC}-Starvation) were also arranged (Grey: EXO_{FBS}-nFBS, Blue: EXOsc-Starvation). The distinction among them was made based on the separation along the first component axis (89.9% of variance) and the second component axis (8.6% of variance), exhibiting a clear separation of the exosome subpopulation according to the contents of UCMSC-derived exosome and FBS-derived exosome. The EXO_{SC}-UF-dFBS is most similar to the EXO_{SC}-Starvation, and EXO_{SC}-UC-dFBS and EXO_{SC}-nFBS have similar characteristics as EXO_{FBS}-nFBS with large amounts of FBS-derived exosomes. These data are correlated with the results that EXO_{SC}-UF-dFBS has the highest purity, as confirmed by impurities detection. FTIR combined with PCA could be a powerful tool to fingerprint exosome subpopulations depending on the ratio of FBS-derived exosome and MSC-derived exosome. The results of zeta potential showed that the EXO_{SC}-UF-dFBS has a similar zeta potential with EXO_{SC}-Starvation, whereas the zeta potential of EXO_{SC}-UC-dFBS indicates similarity with EXO_{FBS}-nFBS due to remaining large number of FBS-derived exosome after depletion process (Figure 5(c)).

The expression of angiogenic factors in UCMSC-derived exosomes

Exosomes represent the characteristics of parent cells by the paracrine effect. As a result of comparing the level of cytokine expression in UCMSC-derived exosomes isolated in various culture conditions, angiogenesis-related cytokine was highly expressed in EXO_{SC}-UF-dFBS. The degree of angiogenic factor expression, related to the characteristics of MSCs, is different based on the ratio of UCMSC-derived exosomes. The protein expression level was compared with ELISA to prove the difference between representative angiogenesis-related cytokines denoted in

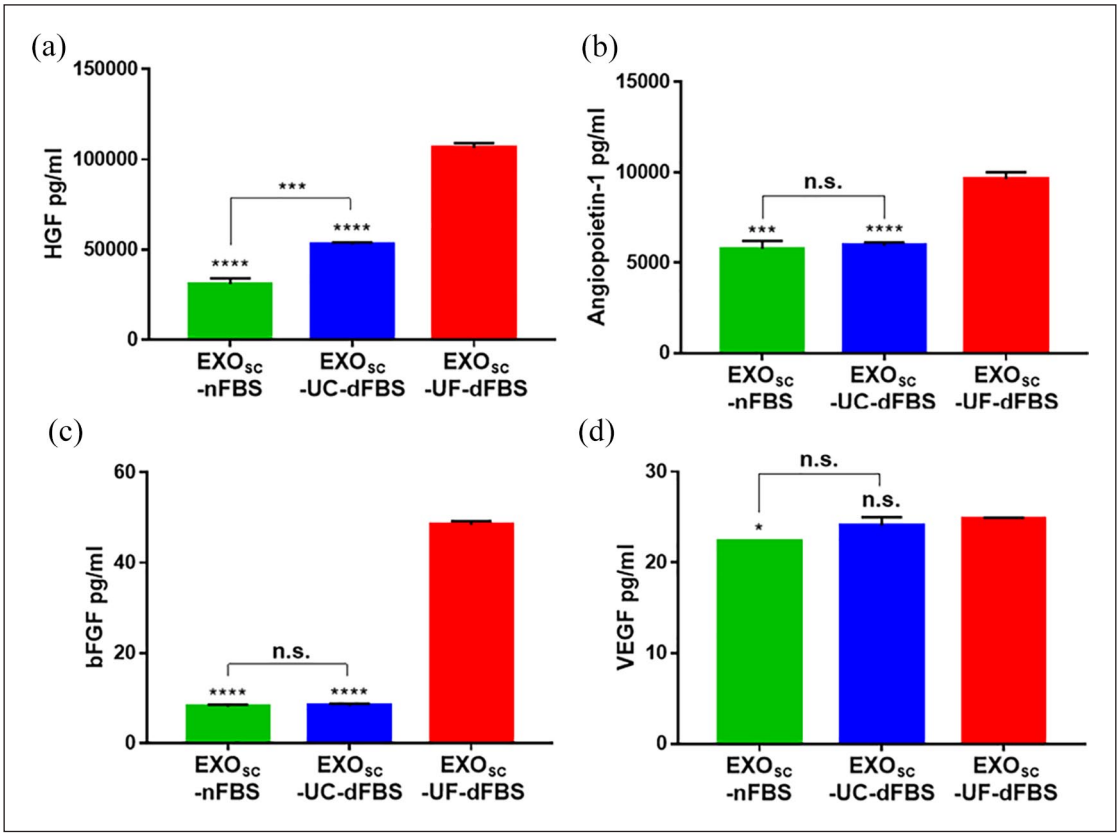

Figure 6. Angiogenic marker protein production on UCMSC-derived exosomes: (a) levels of HGF, (b) Angiopoietin-1, (c) bFGF, and (d) VEGF detected by ELISA in exosome.
Values are presented as mean ± SD ($n = 3$) and statistical significance was obtained with one-way analysis of ANOVA with Tukey's multiple comparison post-test (*$p < 0.05$; ***$p < 0.001$; ****$p < 0.0001$).

cytokine array. Figure 6 shows the protein level of angiogenic factors depending on the ratio of UCMSC-derived exosomes. The expression level of angiogenesis-related factors, HGF, Angiopoietin-1, bFGF, and VEGF increased in EXO_{SC}-UF-dFBS, whereas EXO_{SC}-nFBS and EXO_{SC}-UC-dFBS showed a similar degree of expression (Figure 6(a)–(d)).

The wound healing and angiogenic effects of UCMSC-derived exosome

In order to assess angiogenic effects, facilitated by UCMSC-derived exosomes, we studied exosomes in their ability to induce HCAECs migration during wound healing processes by scratch assay. HCAECs were incubated to be confluent and treated with the same concentration of exosomes derived from FBS, whereas exosomes derived from UCMSC cultured with nFBS, UC-dFBS, and UF-dFBS for 24 h after the creation of scratch. After exosome incubation, the migration rate of HCAECs was increased at all kinds of exosomes compared to cells without exosome treatments. Notably, the EXO_{SC}-UF-dFBS showed significant effects on cell migration, and cell migration increased as there was an increase in contents of UCMSC-derived exosomes (Figure 7(a)). The result of the scratch assay was analyzed by ImageJ after 24 h exosome treated. (Figure 7(b)).

Angiogenesis plays a pivotal role in wound healing, and the pro-angiogenic capability of MSC-derived exosomes has been reported.[44] The tube formation assay is an in vitro model of angiogenesis. Therefore, the activity of exosomes derived from FBS and UCMSC in various conditioned medium was investigated in an in vitro capillary tube formation assay using HCAECs (Figure 7(c)). The total tube length, total branching length, and the number of nodes and junctions at the indicated time were measured to quantify the ability of tube formation depending on the ratio of UCMSC-derived exosome. All parameters of tube formation significantly increased after incubation with EXO_{SC}-UF-dFBS, as compared to EXO_{FBS}-nFBS, EXO_{SC}-nFBS, and EXO_{SC}-UC-dFBS (Figure 7(d)). Taken together, our in vitro functional assays on HCAECs suggested that efficient depletion of

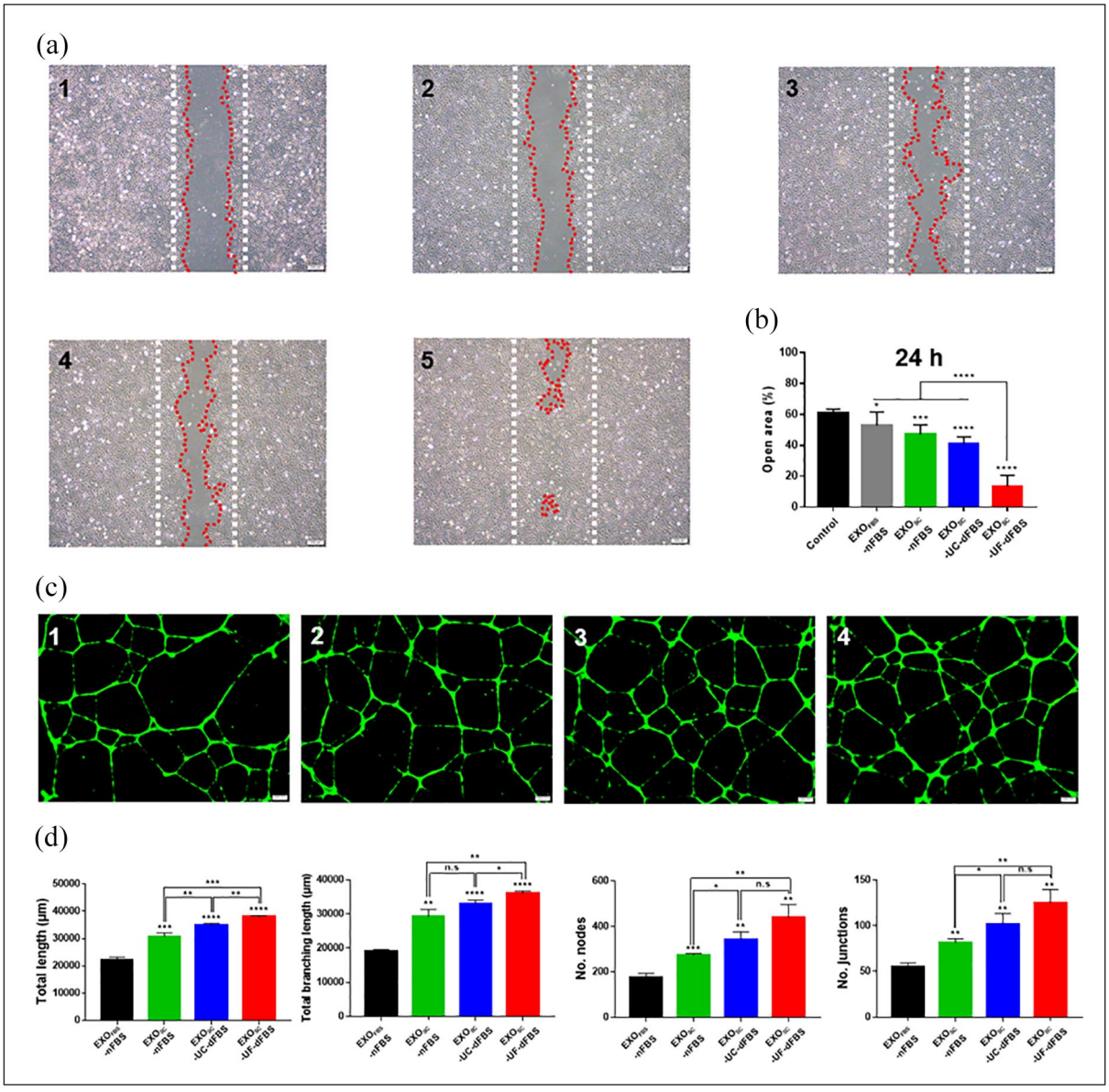

Figure 7. Wound healing and angiogenic effect of MSC-derived exosome: (a) representative images of the cell migration effect of UCMSC-derived exosomes (1: Control; 2: EXO_{FBS}-nFBS; 3: EXO_{SC}-nFBS; 4: EXO_{SC}-UC-dFBS; 5: EXO_{SC}-UF-dFBS), (b) rates of cell migration were quantified using Image J. Scale bars 200 μm, (c) representative images of the angiogenesis effect of UCMSC-derived exosomes (1: EXO_{FBS}-nFBS; 2: EXO_{SC}-nFBS; 3: EXO_{SC}-UC-dFBS; 4: EXO_{SC}-UF-dFBS), and (d) analysis of total length, total branching length, the number of nodes, the number of junctions (analysis with Image J).
Values are presented as mean ± SD ($n = 3$) and statistical significance was obtained with one-way analysis of ANOVA with Tukey's multiple comparison post-test (*$p < 0.05$; **$p < 0.01$; ***$p < 0.001$; ****$p < 0.0001$).

FBS-derived exosomes facilitated wound healing and angiogenic effects of UCMSC-derived exosomes for endothelial cells.

Discussion

Exosome research is growing rapidly due to its excellent biological activity and the potential for clinical applications. In particular, exosomes are focused as new therapeutics that overcome the shortcoming of cell-based therapeutics due to their regenerative properties derived from paracrine effects by exosomes released from stem cells.[45–47] For this reason, it is important to isolate natural exosomes secreted from stem cells, but the current conventional ultracentrifugation-based separation of exosomes requires a lot of labor and time. And the problem is that the

amounts of exosomes obtained through this process are extremely small with aggregation, although the purity is relatively high.[47] Besides, the amount of isolated exosomes is not constant, indicating the need for exosome isolation processes to be standardized.

Another important point is the isolation of highly purified exosomes from specific cells without contaminants. In clinical applications, separating only specific cell-derived exosomes with high purity is an important factor in maximizing therapeutic effects and minimizing side effects. Thus, in recent years, various applications using exosomes have been studied, and basic research on the method of separating exosomes with high yield and purity has been actively carried out.

In this report, we studied to standardize the process from preparation of cell culture medium to isolation methods for exosome from stem cell with high yield and purity. Furthermore, with isolations of highly purified stem cell-derived exosomes, it has been shown that the representative regenerative effects, angiogenesis, and wound healing, can be maximized. The same amounts of cell were used in all experiments to compare the separation efficiency of exosomes depending on various conditions.

The conventional ultracentrifugation (UC) method and tangential flow filtration (TFF)-based method were compared to determine the separation method. Compared to UC, the TFF systems enabled highly efficient exosome isolation in a relatively short time. And, the particles separated using TFF were proved to be exosomes through TEM and Western blot analysis. With this result, the TFF was selected to separate exosomes more efficiently compared to the ultracentrifugation method. The TFF system removes small molecular weight substances by filtering samples with a specific membrane.[30] The separation materials can be adjusted according to the cut-off size of membrane, and eventually, controlled the separation efficiency and purity of exosomes. Although the TFF system has been introduced to overcome the shortcoming of isolation through UC, the separation efficiency and purity based on membrane pore size have not been directly compared to suggest appropriate conditions for exosome isolation. We compared the exosomes isolated using 300 and 500 kDa membranes to suggest a suitable pore size of membrane for exosome isolations. Compared to the 300 kDa membrane, a slightly small amount of exosome was obtained using 500 kDa membrane; however, increased the purity of exosome, determined by dividing the number of particles from the amounts of proteins. This result supports that the impurities smaller than 40 nm can be removed using a 500 kDa membrane. With characterizing the exosomes separated through two types of membranes, the structure and the distribution of exosome surface marker expression were similar. Exosomes isolated through two types of membrane, which have the same properties but only affect the purity, suggesting to use of 500 kDa membrane for further experiments.

Another indicator that can determine the purity of cell-derived exosomes is the contents level of exosomes from FBS used in cell culture. FBS is known to provide nutrients and growth factors for cellular proliferation. Besides, electron microscopy and Western blotting analysis confirmed the presence of exosomes in FBS.[48,49] However, in many cases using exosomes isolated from the cell culture medium, researchers have not paid attention to the fact that the purity of exosomes may vary depending on the presence of FBS. It has recently been recognized that the process for exosome-depletion of FBS is necessary to obtain exosomes from cells of interest without contaminating serum-derived exosomes.[50] The common method is to deplete exosomes from FBS by high-speed centrifugation for a long time. Researchers have shown that a large number of exosomes can be depleted from FBS with about 18 h of ultracentrifugation. A recent report showed that the use of ultrafiltration method with a centrifugal filter was compared with the conventional ultracentrifugation method.[51] Besides, we tried to compare the direct effects of an efficient depletion of FBS-derived exosomes on the separation of cell-derived exosomes and their biological activity. By quantifying the amounts of exosomes after depletion processes, it can be shown that FBS-derived exosomes have been removed more efficiently through ultrafiltration and have a similar effect on the cell viability of cells. Next, UCMSCs were cultured using three different culture medium: normal FBS (nFBS), exosome-depleted FBS using ultracentrifugation (UC-dFBS), and exosome-depleted FBS using ultrafiltration (UF-dFBS), and exosomes were isolated from cell culture medium with TFF system. Exosomes isolated from UCMSC cultured with UF-dFBS had the lowest amounts of total proteins and particles, but the ratio of UCMSC-derived exosomes was the highest. Many FBS-derived exosomes have been removed using ultrafiltration to allow the separation of UCMSC-derived exosomes with high purity. By quantifying CD73 expression, which is a stem cell exosome marker,[52,53] and confirming the concentration of LDL-C, an impurity derived from FBS, from the isolated exosomes, it can be proved that UCMSC-derived exosomes were isolated with high purity using UF-dFBS. Interestingly, ExoView™ results showed that CD9 was more abundant in UCMSC-derived exosomes, whereas CD63 was highly expressed in FBS-derived exosomes. CD9 is known to be participated in endothelial cell migration during in vitro wound repair,[54] and CD63 facilitates myocardial fibrosis by interacting with integrin ß1 through tissue inhibitor of matrix metalloproteinase-1 (TIMP-1) promotion,[55] supporting excellent regeneration effects expected by stem cell-derived exosome with a relative higher CD9 and lower CD63 expressions. It can be seen that the biological

properties of exosomes depend on the expression ratio of tetraspanin interacting with each other.[56] And the differences in expression trends of CD9 and CD63, which affect regenerative abilities, are thought to be one of the various reasons that the biological properties increase as the ratio of MSC-derived exosome increases.

FTIR spectroscopy analysis was used to fingerprint exosome subpopulations based on the ratio of FBS-derived and UCMSC-derived exosomes. We combined FTIR spectroscopy and spectral explorations through chemometric tools (Principal Component Analysis, PCA). Exosome subpopulations can be fingerprinted vertically and horizontally, with varying degrees of accuracy.[36] Through PCA analysis, which is converted using FTIR spectrum that varies in the distribution of proteins and lipids of exosomes, exosomes can be classified based on the ratio of FBS-derived and UCMSC-derived exosomes. Exosomes isolated from UCMSC using nFBS (EXO_{SC}-nFBS) and UC-dFBS (EXO_{SC}-UC-dFBS) showed similar properties to FBS-derived exosomes (EXO_{FBS}), whereas exosomes isolated from UCMSC using UF-dFBS (EXO_{SC}-UF-dFBS) exhibited similarity with UCMSC-derived exosome in starvation condition (EXO_{SC}-Starvation). Zeta potential is an indispensable factor for determining the distinction and dispersion stability of exosomes.[57] Exosomes isolated from different exosome depleted FBS mediums displayed negative charges ranged from −25.4 to −18.0 mV with high dispersion stability. Using zeta potential analysis, exosomes could be classified depending on the ratio of UCMSC derived and FBS-derived exosomes. The EXO_{SC}-UF-dFBS has a similar zeta potential with EXO_{SC}-Starvation, whereas the zeta potential of EXO_{SC}-UC-dFBS indicates similarity with EXO_{FBS}-nFBS due to remaining large number of FBS-derived exosome after depletion process.

Cytokine array was performed based on the ratio of UCMSC-derived exosomes to obtain a preliminary profile of angiogenic factors presenting in exosomes. The results demonstrated that the different expression level of angiogenic factors was significantly related to the contents of exosomes derived from UCMSC. Four different angiogenic factors were selected and analyzed the expression level of protein using ELISA depending on the results of cytokine array. The ELISA results also support that the various angiogenic factors were expressed in the UCMSC-derived exosome compared to FBS-derived exosomes. Finally, the wound healing and angiogenic effects of UCMSC-derived exosomes were verified using in vitro assays with same amounts of exosome based on the protein concentration (100 µg/ml).[58,59] All parameters related to tube formation increased as the purity of UCMSC-derived exosomes, and the purity of cell-derived exosomes is essential to maximize the effect of exosomes with the same concentration.

Conclusion

Overall, we proposed a method to increase the purity of exosomes derived from specific cells through an optimization process with comparative experiments from cell culture medium preparation to exosome isolation. Furthermore, the possibility of maximizing the regeneration effect through highly purified stem cell-derived exosomes is shown using cell migration and tube formation assays. Our comparative study expects standardization of the MSC-derived exosome isolation processes with high yield and purity for successful clinical applications without any side effect derived from impurities.

Declaration of conflicting interests

The author(s) declared no potential conflicts of interest with respect to the research, authorship, and/or publication of this article.

Funding

The author(s) disclosed receipt of the following financial support for the research, authorship, and/or publication of this article: This work was supported by Basic Science Research Program (2017R1A6A3A04012362 and 2020R1A2B5B03002344) and Bio & Medical Technology Development Program (2018M 3A9E2024579) through the National Research Foundation of Korea funded by the Ministry of Science and ICT (MSIT), and the Korea Medical Device Development Fund grant funded by the Korea government (the Ministry of Science and ICT, the Ministry of Trade, Industry and Energy, the Ministry of Health & Welfare, Republic of Korea, the Ministry of Food and Drug Safety) (202011A05-05), Republic of Korea.

ORCID iDs

Da-Seul Kim https://orcid.org/0000-0002-6281-0434
Dong Keun Han https://orcid.org/0000-0001-9015-9071

Supplemental material

Supplemental material for this article is available online.

References

1. Lee DJ, Kwon J, Current L, et al. Osteogenic potential of mesenchymal stem cells from rat mandible to regenerate critical sized calvarial defect. *J Tissue Eng* 2019; 10: 2041731419830427.
2. Lou G, Chen Z, Zheng M, et al. Mesenchymal stem cell-derived exosomes as a new therapeutic strategy for liver diseases. *Exp Mol Med* 2017; 49: e346.
3. Gao F, Chiu S, Motan D, et al. Mesenchymal stem cells and immunomodulation: current status and future prospects. *Cell Death Dis* 2016; 7: e2062.
4. Pittenger MF, Discher DE, Péault BM, et al. Mesenchymal stem cell perspective: cell biology to clinical progress. *NPJ Regen Med* 2019; 4: 22.

5. Le H, Xu W, Zhuang X, et al. Mesenchymal stem cells for cartilage regeneration. *J Tissue Eng* 2020; 11: 2041731420943839.
6. Baraniak PR and McDevitt TC. Stem cell paracrine actions and tissue regeneration. *Regen Med* 2010; 5: 121–143.
7. Jin Q, Li P, Yuan K, et al. Extracellular vesicles derived from human dental pulp stem cells promote osteogenesis of adipose-derived stem cells via the MAPK pathway. *J Tissue Eng* 2020; 11: 2041731420975569.
8. Patel DB, Gray KM, Santharam Y, et al. Impact of cell culture parameters on production and vascularization bioactivity of mesenchymal stem cell-derived extracellular vesicles. *Bioeng Transl Med* 2017; 2: 170–179.
9. Liang X, Ding Y, Zhang Y, et al. Paracrine mechanisms of mesenchymal stem cell-based therapy: current status and perspectives. *Cell Transplant* 2014; 23: 1045–1059.
10. Lai RC, Chen TS and Lim SK. Mesenchymal stem cell exosome: a novel stem cell-based therapy for cardiovascular disease. *Regen Med* 2011; 6: 481–492.
11. Yáñez-Mó M, Siljander PR-M, Andreu Z, et al. Biological properties of extracellular vesicles and their physiological functions. *J Extracell Vesicles* 2015; 4: 27066.
12. Valadi H, Ekström K, Bossios A, et al. Exosome-mediated transfer of mRNAs and microRNAs is a novel mechanism of genetic exchange between cells. *Nat Cell Biol* 2007; 9: 654–659.
13. Rostom DM, Attia N, Khalifa HM, et al. The therapeutic potential of extracellular vesicles versus mesenchymal stem cells in liver damage. *Tissue Eng Regen Med* 2020; 17: 537–552.
14. Théry C, Witwer KW, Aikawa E, et al. Minimal information for studies of extracellular vesicles 2018 (MISEV2018): a position statement of the International Society for Extracellular Vesicles and update of the MISEV2014 guidelines. *J Extracell Vesicles* 2018; 7: 1535750.
15. Battistelli M and Falcieri E. Apoptotic bodies: particular extracellular vesicles involved in intercellular communication. *Biology (Basel)* 2020; 9: 21.
16. Lener T, Gimona M, Aigner L, et al. Applying extracellular vesicles based therapeutics in clinical trials–an ISEV position paper. *J Extracell Vesicles* 2015; 4: 30087.
17. Russell AE, Sneider A, Witwer KW, et al. Biological membranes in EV biogenesis, stability, uptake, and cargo transfer: an ISEV position paper arising from the ISEV membranes and EVs workshop. *J Extracell Vesicles* 2019; 8: 1684862.
18. Vlassov AV, Magdaleno S, Setterquist R, et al. Exosomes: current knowledge of their composition, biological functions, and diagnostic and therapeutic potentials. *Biochim Biophys Acta* 2012; 1820: 940–948.
19. Hu L, Wang J, Zhou X, et al. Exosomes derived from human adipose mensenchymal stem cells accelerates cutaneous wound healing via optimizing the characteristics of fibroblasts. *Sci Rep* 2016; 6: 32993.
20. Bian X, Ma K, Zhang C and Fu X. Therapeutic angiogenesis using stem cell-derived extracellular vesicles: an emerging approach for treatment of ischemic diseases. *Stem Cell Res Ther* 2019; 10: 158.
21. Bruno S, Chiabotto G and Camussi G. Extracellular vesicles: a therapeutic option for liver fibrosis. *Int J Mol Sci* 2020; 21: 4255.
22. Han C, Zhou J, Liang C, et al. Human umbilical cord mesenchymal stem cell derived exosomes encapsulated in functional peptide hydrogels promote cardiac repair. *Biomater Sci* 2019; 7: 2920–2933.
23. Asil SM, Ahlawat J, Barroso GG, et al. Nanomaterial based drug delivery systems for the treatment of neurodegenerative diseases. *Biomater Sci* 2020; 8: 4109–4128.
24. Toh WS, Lai RC, Hui JHP, et al. MSC exosome as a cell-free MSC therapy for cartilage regeneration: implications for osteoarthritis treatment. *Semin Cell Dev Biol* 2017; 67: 56–64.
25. Gardiner C, Vizio DD, Sahoo S, et al. Techniques used for the isolation and characterization of extracellular vesicles: results of a worldwide survey. *J Extracell Vesicles* 2016; 5: 32945.
26. Furi I, Momen-Heravi F and Szabo G. Extracellular vesicle isolation: present and future. *Ann Transl Med* 2017; 5: 263.
27. Gámez-Valero A, Monguió-Tortajada M, Carreras-Planella L, et al. Size-Exclusion Chromatography-based isolation minimally alters Extracellular Vesicles' characteristics compared to precipitating agents. *Sci Rep* 2016; 6: 33641.
28. Yang D, Zhang W, Zhang H, et al. Progress, opportunity, and perspective on exosome isolation-efforts for efficient exosome-based theranostics. *Theranostics* 2020; 10: 3684.
29. Busatto S, Giacomini A, Montis C, et al. Uptake profiles of human serum exosomes by murine and human tumor cells through combined use of colloidal nanoplasmonics and flow cytofluorimetric analysis. *Anal Chem* 2018; 90: 7855–7861.
30. Busatto S, Vilanilam G, Ticer T, et al. Tangential flow filtration for highly efficient concentration of extracellular vesicles from large volumes of fluid. *Cells* 2018; 7: 273.
31. van Reis R, Gadam S, Frautschy LN, et al. High performance tangential flow filtration. *Biotechnol Bioeng* 1997; 56: 71–82.
32. Helwa I, Cai J, Drewry MD, et al. A comparative study of serum exosome isolation using differential ultracentrifugation and three commercial reagents. *PLoS One* 2017; 12: e0170628.
33. Rekker K, Saare M, Roost AM, et al. Comparison of serum exosome isolation methods for microRNA profiling. *Clin Biochem* 2014; 47: 135–138.
34. Karimi N, Cvjetkovic A, Jang SC, et al. Detailed analysis of the plasma extracellular vesicle proteome after separation from lipoproteins. *Cell Mol Life Sci* 2018; 75: 2873–2886.
35. Lobb RJ, Becker M, Wen Wen S, et al. Optimized exosome isolation protocol for cell culture supernatant and human plasma. *J Extracell Vesicles* 2015; 4: 27031.
36. Paolini L, Federici S, Consoli G, et al. Fourier-transform Infrared (FT-IR) spectroscopy fingerprints subpopulations of extracellular vesicles of different sizes and cellular origin. *J Extracell Vesicles* 2020; 9: 1741174.
37. Gualerzi A, Kooijmans SAA, Niada S, et al. Raman spectroscopy as a quick tool to assess purity of extracellular vesicle preparations and predict their functionality. *J Extracell Vesicles* 2019; 8: 1568780.
38. Son KK, Tkach D and Rosenblatt J. Delipidated serum abolishes the inhibitory effect of serum on *in vitro* liposome-mediated transfection. *Biochim Biophys Acta* 2001; 1511: 201–205.

39. Ollesch J, Drees SL, Heise HM, et al. FTIR spectroscopy of biofluids revisited: an automated approach to spectral biomarker identification. *Analyst* 2013; 138: 4092–4102.
40. Barth A. Infrared spectroscopy of proteins. *Biochim Biophys Acta* 2007; 1767: 1073–1101.
41. Casal HL and Mantsch HH. Polymorphic phase behaviour of phospholipid membranes studied by infrared spectroscopy. *Biochim Biophys Acta* 1984; 779: 381–401.
42. Zlotogorski-Hurvitz A, Dekel BZ, Malonek D, et al. FTIR-based spectrum of salivary exosomes coupled with computational-aided discriminating analysis in the diagnosis of oral cancer. *J Cancer Res Clin Oncol* 2019; 145: 685–694.
43. Mihály J, Deák R, Szigyártó IC, et al. Characterization of extracellular vesicles by IR spectroscopy: fast and simple classification based on amide and CH stretching vibrations. *Biochim Biophys Acta Biomembr* 2017; 1859: 459–466.
44. Zhang B, Wu X, Zhang X, et al. Human umbilical cord mesenchymal stem cell exosomes enhance angiogenesis through the Wnt4/β-catenin pathway. *Stem Cells Transl Med* 2015; 4: 513–522.
45. Zhang ZG, Buller B and Chopp M. Exosomes—beyond stem cells for restorative therapy in stroke and neurological injury. *Nat Rev Neurol* 2019; 15: 193–203.
46. Ibrahim AG-E, Cheng K and Marbán E. Exosomes as critical agents of cardiac regeneration triggered by cell therapy. *Stem Cell Rep* 2014; 2: 606–619.
47. Ludwig N, Whiteside TL and Reichert TE. Challenges in exosome isolation and analysis in health and disease. *Int J Mol Sci* 2019; 20: 4684.
48. Shelke GV, Lässer C, Gho YS, et al. Importance of exosome depletion protocols to eliminate functional and RNA-containing extracellular vesicles from fetal bovine serum. *J Extracell Vesicles* 2014; 3: 24783.
49. Théry C, Amigorena S, Raposo G, et al. Isolation and characterization of exosomes from cell culture supernatants and biological fluids. *Curr Protoc Cell Biol* 2006; Chapter 3: Unit 3.22.
50. Aswad H, Jalabert A and Rome S. Depleting extracellular vesicles from fetal bovine serum alters proliferation and differentiation of skeletal muscle cells *in vitro*. *BMC Biotechnol* 2016; 16: 32.
51. Kornilov R, Puhka M, Mannerström B, et al. Efficient ultrafiltration-based protocol to deplete extracellular vesicles from fetal bovine serum. *J Extracell Vesicles* 2018; 7: 1422674.
52. Ramos TL, Sánchez-Abarca LI, Muntión S, et al. MSC surface markers (CD44, CD73, and CD90) can identify human MSC-derived extracellular vesicles by conventional flow cytometry. *Cell Commun Signal* 2016; 14: 2.
53. Secco M, Moreira YB, Zucconi E, et al. Gene expression profile of mesenchymal stem cells from paired umbilical cord units: cord is different from blood. *Stem Cell Rev Rep* 2009; 5: 387–401.
54. Klein-Soyer C, Azorsa DO, Cazenave J-P, et al. CD9 participates in endothelial cell migration during *in vitro* wound repair. *Arterioscler Thromb Vasc Biol* 2000; 20: 360–369.
55. Takawale A, Zhang P, Patel VB, et al. Tissue inhibitor of matrix metalloproteinase-1 promotes myocardial fibrosis by mediating CD63–integrin β1 interaction. *Hypertension* 2017; 69: 1092–1103.
56. Radford KJ, Thorne RF and Hersey P. CD63 associates with transmembrane 4 superfamily members, CD9 and CD81, and with β1 integrins in human melanoma. *Biochem Biophys Res Commun* 1996; 222: 13–18.
57. Bhattacharjee S. DLS and zeta potential–what they are and what they are not? *J Control Release* 2016; 235: 337–351.
58. Xue C, Shen Y, Li X, et al. Exosomes derived from hypoxia-treated human adipose mesenchymal stem cells enhance angiogenesis through the PKA signaling pathway. *Stem Cells Dev* 2018; 27: 456–465.
59. Gong M, Yu B, Wang J, et al. Mesenchymal stem cells release exosomes that transfer miRNAs to endothelial cells and promote angiogenesis. *Oncotarget* 2017; 8: 45200–45212.